

FA-SCANSAR: FULL APERTURE SCANNING PULSE BY PULSE FOR THE NEARSPACE SLOW-MOVING PLATFORM BORNE SAR

B. Sun, J. Chen, C.-S. Li, and Y.-Q. Zhou

School of Electronics and Information Engineering
Beijing University of Aeronautics and Astronautics
No. 37, Xueyuan Road, Haidian District, Beijing 100191, China

Abstract—Because the nearspace slow-moving platform borne synthetic aperture radar (SAR) can realize high resolution imaging using low pulse repetition frequency (PRF), a full-aperture ScanSAR (FA-ScanSAR) operation, which switches the range beam pulse by pulse, was proposed for wide swath imaging. This operation separates the wide swath into several sub-swaths, and each of which can be illuminated by a narrow range beam. The SAR antenna switches the range beam to point at each of the sub-swaths in turn, transmits pulses and receives echoes pulse by pulse. The design method of main system parameters and the calculating expressions of the performance indexes are addressed in the paper. A design example is given to compare the performance of the conventional strip operation, ScanSAR and FA-ScanSAR operation. The results show that FA-ScanSAR operation can obtain high resolution by full aperture accumulation in wide swath and improve the signal-to-noise ratio of SAR images for the nearspace slow-moving platform borne SAR.

1. INTRODUCTION

High resolution and wide swath are the two important aspects of synthetic aperture radar (SAR), but conventional SAR systems suffer from limitations in resolution and swath width [1–3]. One usually has some trade-off between the two [4] according to the system task. In contrast to the conventional strip operation, ScanSAR [5] and TOPSAR [6] achieve wider swath at the expense of degraded azimuth

resolution and can be utilized for effectively general observation. Spotlight operation [7] has a better resolution but smaller and discontinuous imaging area. Several techniques were presented to solve the contracting. Multiple beams systems in azimuth or/and range are the two solutions of them. Single-transmitting multiple-receiving by multiple beams in azimuth [6–10] can obtain wider swath with the same azimuth resolution, but it is hard to compensate the inconsistency of channels and non-uniform sampling. Single-transmitting multiple-receiving with multiple beams in elevation can achieve the same effect, but the interference of the neighbor beams and the gaps between the neighbor swaths exist. Another problem for multiple beams systems is the increasing complexity for system realization as the number of channels increases. Recent years, SweepSAR is a novel operation presented by NASA DESDynl [11] Team, which replaces complex beam-forming networks by a reflector-phased array feed combination for spaceborne SAR [4]. It can receive echoes of several subswaths with a sweeping beam in range. This operation is utilized for ecosystems, solid earth and cryosphere science. The resolution is not very high. However, the swath width is larger than that of convention operation at the same resolution.

Nearspace (the altitude between 18 km and 100 km), the region between controlled commercial airspace and LEO, offers new capabilities not accessible to orbiting satellites or maneuvering aircraft-capabilities critical to emerging national defense needs [12]. Two typical kinds of platforms have been researched in recent years. One is the huge-volume slow-moving platform, e.g., High Altitude Airship (HAA) [13], and the other is ultrasonic aircraft, e.g., FALCON [14]. And the nearspace SAR has been becoming a revolutionizing remote sensing mission [15]. Recently most researches [15–17] have concentrated on the ultrasonic aircrafts borne SAR because the SAR system parameters of them are similar to those of conventional airborne SAR, and the traditional SAR techniques can be extended to the ultrasonic aircrafts. In contrast to the ultrasonic aircrafts, for the slow-moving platform borne SAR, it is too hard to compensate the motion errors because of the long aperture time caused by the slow velocity. However, it has an important advantage that high resolution and wide swath imaging can be achieved without the conditionality of pulse repetition frequency (PRF) and swath width. As high resolution can be obtained with small Doppler bandwidth due to the slow platform velocity, a lower azimuth sample rate (PRF) can be chosen, and a swath width up to thousands of kilometers can be achieved, which is mainly determined by the sight distance and power supply. Therefore, high resolution and wide swath are theoretically feasible if the range

beam width is wide enough. Unfortunately the wide beam cannot supply enough gain, so the transmit power demand will be beyond the practical supply. In this paper, a full aperture scanning operation with a single range narrow beam called FA-ScanSAR is proposed to resolve this problem. The two advantages of it are: 1) A range narrow beam can obtain enough gain; 2) The scanning to each sub-swath pulse by pulse can obtain full aperture accumulation, resulting in higher imaging processing gain and better resolution than conventional ScanSAR.

The second section of this paper discusses the FA-ScanSAR principle, and the main system parameters design methods and performance calculation expressions are analyzed in the third section. Then a design example is given to illustrate the parameters design and compare the performance differences of conventional strip operation, ScanSAR and FA-ScanSAR operation. Finally, it is concluded that FA-ScanSAR is a feasible operation for high resolution and wide swath imaging for the nearspace slow-moving platform SAR.

2. FA-SCANSAR PRINCIPLE

Based on the basic theory of SAR, the azimuth resolution expression is

$$\delta_a = k_1 \frac{v}{B_a} \quad (1)$$

where k_1 , v , B_a are the azimuth broadening index, the platform's velocity and Doppler bandwidth respectively. Generally, pulse repetition frequency f_p can be chosen a little greater than Doppler bandwidth. That is

$$f_p = k_p B_a \quad (2)$$

where k_p is the oversampling factor and usually equals 1.1 ~ 1.2. Then,

$$\delta_a = k_1 k_p \frac{v}{f_p} \quad (3)$$

If the azimuth resolution is lower than 1.0 m, for spaceborne SAR, PRF is usually greater than 8000 Hz, and the slant range width is no more than 20 km since the satellite's velocity is about 7000 m/s. For the nearspace slow-moving platform borne SAR, if the platform's velocity is less than 50 m/s, PRF can be chosen at several tens of Hz, and the calculated slant range can be up to thousands of kilometers according to the pulse repetition interval. The main restrictions of actual swath width are the radar geometry relationship and power supply instead of PRF. So it is possible to achieve high resolution and wide swath imaging for the nearspace slow-moving platform.

Another difficulty for high resolution and wide swath imaging is the large transmit power demand. Generally, the signal-to-noise ratio (SNR) of SAR images of strip SAR is

$$\text{SNR} = \frac{P_t G_t G_r \lambda^2 \sigma_o \delta_a \delta_r}{(4\pi)^3 R^4 F k T_n B_w} \cdot k_a f_p T_s \cdot k_r B_w \tau_p \quad (4)$$

where P_t is the peak power of transmitted signal. G_t and G_r are the antenna gain on transmit and receive respectively. λ is the wavelength. σ_o is the normalized radar cross section of the target. δ_a and δ_r are the azimuth and range resolution. R is the target slant range. F is the system loss. k is Boltzmann's constant, T_n the noise temperature, B_w the bandwidth of the processor, τ_p the transmitting pulse length, and T_s the signal accumulate time. k_a and k_r are the non-ideal gain factors on azimuth and range due to windowing and other processing. The last two terms of the expression are the imaging processing gain on azimuth and range.

Based on the antenna theory, the antenna gain [1] is

$$G = \rho \frac{4\pi L_a L_r}{\lambda^2} \approx \rho \frac{4\pi}{\beta_a \beta_r} \quad (5)$$

where ρ is the antenna efficiency. L_a and L_r are the antenna length in azimuth and range respectively. β_a and β_r are the antenna beamwidth in azimuth and range respectively. So if a wide beam in range is used for wide swath imaging, the antenna gain is very low, and the SNR is very low. Single-transmitting multiple-receiving with multiple beams in elevation can improve several dBs on SNR, but for wide swath imaging, it is not enough. For ScanSAR operation, due to the increased resolution, SNR of ScanSAR image is better than that of the conventional strip operation even if the azimuth processing gain is lower.

The basic thought of FA-ScanSAR is: To separate the wide swath into N subswaths, each of them works in conventional strip operation at the same time. The differences are that the actual PRF becomes N times of the original, and the SAR switches the beam to point at each subswath pulse by pulse, transmits the pulse and receives the echo of the current subswath, then switches to point at another subswath.

Figure 1 gives an example of FA-ScanSAR with 4 subswaths. The whole wide swath is divided into 4 subswaths. A narrower beam points at the first subswath at first, then the SAR transmits one pulse and receives one echo of the first subswath, and then switches the beam to point at the second swath, transmits one pulse and receives one echo of the second subswath, and switches the beam back to the first subswath until the echo of the fourth subswath is recorded. The time duration

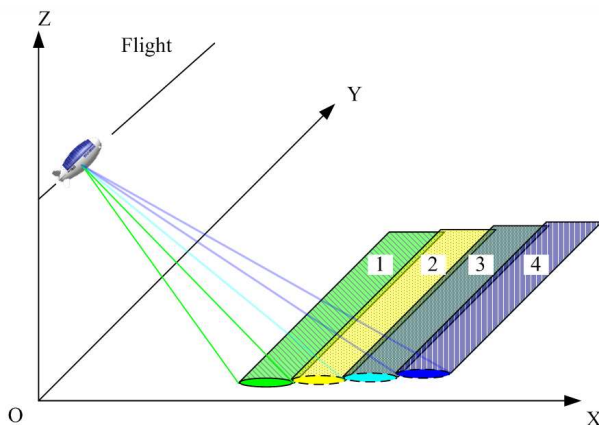


Figure 1. Sketch map of FA-ScanSAR with 4 subswaths.

of the processes, including four times switching pointing, transmitting pulse and receiving echo, is a period of scanning. To avoid the gaps between the subswaths, the overlap must be considered.

The difference between ScanSAR and FA-ScanSAR is that ScanSAR switches the beam to a subswath and transmits a few pulses and receives the same number of echoes in a burst time; FA-ScanSAR switches the range beam in every pulse, transmits one pulse and receives one echo in a period. The benefit is that FA-ScanSAR can illustrate targets in a full aperture time and achieve high resolution in wide swath. The continual beam switch is the main characteristic and key technique for FA-ScanSAR operation. Fortunately, the nearspace slow-moving platform SAR can use low PRF. There is enough time to switch the beam, transmit pulse and receive echo by a high performance phase control array antenna. So it is practical to realize high resolution and wide swath imaging with a single-transmitting single-receiving SAR system in FA-ScanSAR operation.

Based on the principle of FA-ScanSAR, the work schedule of transmitting pulse and receiving echo can be given. Figure 2 displays a whole period T , which is equal to the conventional strip operation with a wide beam, with $N = 4$ subswaths. For subswath i , the time T_i is divided into four slices: The length of current transmitted pulse τ_{p_i} , echo delay T_{d_i} , echo window length T_{w_i} , beam switch and preparing time T_{f_i} . In fact, τ_{p_i} , T_{d_i} , T_{w_i} and T_{f_i} can be different from those of other subswaths, and the expense is the increased complexity in control. If the differences of the time parameters for all subswaths are neglected, the time schedule of FA-ScanSAR is equivalent to that

of the conventional strip with N times PRF.

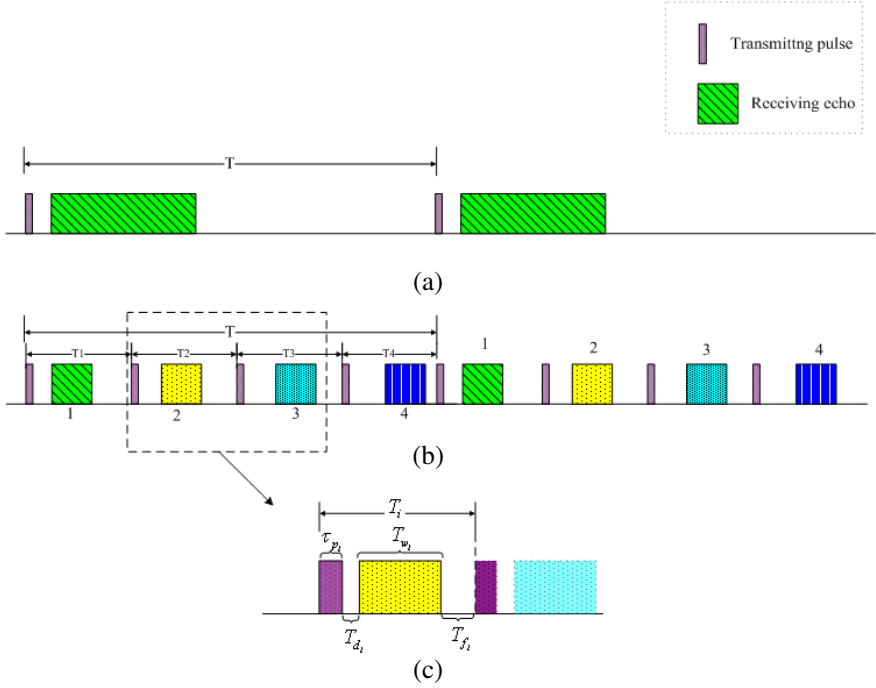


Figure 2. Work schedule. (a) Conventional strip operation with a wide beam, (b) FA-ScanSAR operation with 4 subswaths, (c) time decomposition of a subswath.

According to the principle and time schedule, if the ambiguous signals between the subswath are neglected, the dataset of each subswath is independent. And the data subtracted one sample from N sample in azimuth can be processed by conventional strip imaging algorithms. The corresponding pulse repetition time is T instead of T_i . After cutting the overlap area, the mosaic image can be formed. In contrast to ScanSAR operation, the time interval of the azimuth pixel is the same, and there is no scalloping effect, so the imaging process is much easier.

3. SYSTEM PARAMETERS DESIGN FOR FA-SCANSAR

3.1. Subswath Number

The subswath number is calculated by the system azimuth resolution δ_a , swath width Δ and look angle of the central swath θ . The calculating steps are as follows:

a. Calculate the minimum PRF $f_{p\min}$ from the system azimuth resolution δ_a , the velocity of the platform v . According to (3), the minimum PRF $f_{p\min}$ is

$$f_{p\min} = k_1 k_p \frac{v}{\delta_a} \quad (6)$$

Generally, the azimuth ambiguity gets better as PRF increases. So the available PRF should increase from above until the azimuth ambiguities-to-signal ratio (AASR) is acceptable.

b. Calculate the maximum PRF $f_{p\max}$ based on the geometry. The parameters labeled in Figure 3 can be calculated by the following expressions. The look angle of the central swath θ , the earth radius R_e and the height of the platform h are given.

$$R = R_h \cos \theta - \sqrt{R_e^2 - R_h^2 \sin^2 \theta} \quad (7)$$

$$\alpha = \text{asin} \left(\frac{R \sin \theta}{R_e} \right) \quad (8)$$

$$g_{\min} = R_e \text{asin} \left(\frac{R \sin \theta}{R_e} \right) - \frac{\Delta}{2} \quad (9)$$

$$\alpha_{\min} = \text{asin} \left(\frac{R \sin \theta}{R_e} \right) - \frac{\Delta}{2R_e} \quad (10)$$

$$\alpha_{\max} = \text{asin} \left(\frac{R \sin \theta}{R_e} \right) + \frac{\Delta}{2R_e} \quad (11)$$

$$R_{\min} = \sqrt{R_h^2 + R_e^2 - 2R_h R_e \cos \alpha_{\min}} \quad (12)$$

$$R_{\max} = \sqrt{R_h^2 + R_e^2 - 2R_h R_e \cos \alpha_{\max}} \quad (13)$$

Based on the time schedule in Figure 2, we can get

$$T = \frac{1}{f_p} \geq \tau_p + \frac{2R_{\max}}{c} \quad (14)$$

Then the maximum PRF $f_{p\max}$ is

$$f_{p\max} = \frac{c}{c\tau_p + 2R_{\max}} \quad (15)$$

c. According to $f_{p\max}$ and $f_{p\min}$, the maximum number of subswath N_{\max} is

$$N_{\max} = \lfloor f_{p\max}/f_{p\min} \rfloor \quad (16)$$

where $\lfloor f_{p\max}/f_{p\min} \rfloor$ expresses the maximum integer no greater than $f_{p\max}/f_{p\min}$.

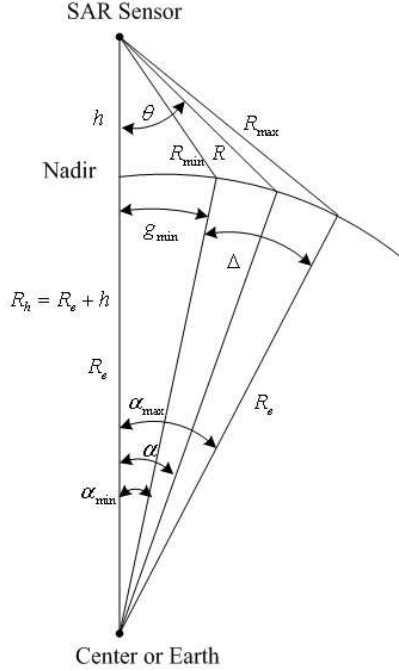


Figure 3. Geometry of SAR sensor and the earth.

The complexity of hardware's implementation will increase as the subswath number increases. So a suitable subswath number N_{opt} needs to be chosen, and the corresponding PRF is $f_{popt} \approx N_{opt} \cdot f_{p\min}$.

3.2. Look Angle and Beam Width of Subswath

Divide the whole swath into N_{opt} subswaths, whose width is the same, and the overlaps between the neighbor subswath are 10% of the width of the subswath Δ_i . Then Δ_i satisfies the equation

$$N_{opt} \cdot \Delta_i - (N_{opt} - 1) \cdot 0.1 \cdot \Delta_i = \Delta \quad (17)$$

where the subscript i represents the subswath sequence number, and $1 \leq i \leq N_{opt}$, $\Delta_1 = \Delta_2 = \dots = \Delta_{N_{opt}}$.

According to the geometry in Figure 3, the ground range $g_{i_{\min}} \sim g_{i_{\max}}$, the earth center angle $\alpha_{i_{\min}} \sim \alpha_{i_{\max}}$, and the slant range $R_{i_{\min}} \sim R_{i_{\max}}$ of the i th subswath can be calculated from the given minimum ground range g_{\min} and the width of subswath Δ_i .

$$g_{i_{\min}} \approx g_{\min} + i \cdot 0.9 \cdot \Delta_i \quad (18)$$

$$g_{i_{\max}} \approx g_{i_{\min}} + \Delta_i \quad (19)$$

$$\alpha_{i_{\min}} = \frac{g_{i_{\min}}}{R_e} \quad (20)$$

$$\alpha_{i_{\max}} = \frac{g_{i_{\max}}}{R_e} \quad (21)$$

$$R_{i_{\min}} = \sqrt{R_h^2 + R_e^2 - 2R_h R_e \cos \alpha_{i_{\min}}} \quad (22)$$

$$R_{i_{\max}} = \sqrt{R_h^2 + R_e^2 - 2R_h R_e \cos \alpha_{i_{\max}}} \quad (23)$$

Then the expressions of the look angle range $\theta_{i_{\min}} \sim \theta_{i_{\max}}$ and central look angle $\theta_{i_{mid}}$ are

$$\theta_{i_{\min}} = \text{asin} \frac{R_e \sin \alpha_{i_{\min}}}{R_{i_{\min}}} \quad (24)$$

$$\theta_{i_{\max}} = \text{asin} \frac{R_e \sin \alpha_{i_{\max}}}{R_{i_{\max}}} \quad (25)$$

$$\theta_{i_{mid}} = \frac{1}{2} (\theta_{i_{\min}} + \theta_{i_{\max}}) \quad (26)$$

3.3. Time Parameters of Subswath

As to the i th subswath, the time slices T_i , τ_{p_i} , T_{d_i} , T_{w_i} and T_{f_i} satisfy the following expressions.

$$T_i = \tau_{p_i} + T_{d_i} + T_{w_i} + T_{f_i} = \frac{1}{f_{p_{opt}}} \quad (27)$$

$$\tau_{p_i} + T_{d_i} \leq \frac{2R_{i_{\min}}}{c} \quad (28)$$

$$T_{w_i} \geq \frac{2(R_{i_{\max}} - R_{i_{\min}})}{c} \quad (29)$$

4. PERFORMANCE ANALYSIS

4.1. Azimuth Resolution and Range Resolution

From the principle of FA-ScanSAR, we can see the subswath is equivalent to that of a conventional strip. If the azimuth beam widths

for all the subswaths are the same, the azimuth resolutions of all the subswaths are the same too, which are equal to $\lambda/2\beta$, where β is the azimuth antenna beamwidth. The azimuth pixel intervals are the same and equal to vT , where v is the platform's velocity, and T is a whole period of scanning.

The range resolution of FA-ScanSAR is similar to that of the conventional strip operation. The slant range resolution is determined by the bandwidth of the transmitting signal, and the ground range resolution is the slant range resolution divided by the sine of incidence angle.

4.2. AASR and RASR

The ambiguous signals include the azimuth and range ambiguities. AASR of FA-ScanSAR is similar to that of conventional strip operation. The difference is that the calculation PRF f_p of each subswath is the actual PRF divided by the subswath number.

$$\text{AASR}_i = \frac{\sum_{\substack{m=-\infty \\ m \neq 0}}^{m=+\infty} \int_{-B_a/2}^{B_a/2} G_{ai}^2(f - f_{dc} + m \cdot f_p) df}{\int_{-B_a/2}^{B_a/2} G_{ai}^2(f - f_{dc}) df} \quad (30)$$

where $G_{ai}(f)$ is the Doppler expression of the azimuth antenna of the i th subswath, and f_{dc} is the corresponding Doppler centroid of the i th subswath.

Range ambiguities-to-signal ratio (RASR) of FA-ScanSAR is different from that of the conventional strip SAR, because the interference of other subswaths must be considered, and the antenna gains of transmitting and receiving antennas are different too.

Let the slant range R be located in the i th subswath, and the slant range of the k th ambiguous area of the m th subswath is

$$R_{ikm} = R + \frac{c}{2} \left[\frac{(m - i)}{f_{p_{opt}}} + \frac{N_{opt}k}{f_{p_{opt}}} \right] \quad (31)$$

According to the geometry in Figure 3,

$$h \leq R_{ikm} \leq \sqrt{R_h^2 - R_c^2} \quad (32)$$

And the ambiguous index range can be calculated, i.e., $k \in [-k_{im1}, k_{im2}]$, where k_{im1} and k_{im2} are integers satisfying (31) and (32). Then the corresponding look angle θ_{ikm} , incidence angle γ_{ikm} , the normalized gain of the transmit antenna $G_{T_{ikm}}$ and the normalized

gain of the receive antenna $G_{R_{ikm}}$ can be calculated by the following expressions.

$$\theta_{ikm} = \text{acos} \left[\frac{R_{ikm}^2 + R_h^2 - R_e^2}{2R_{ikm}R_h} \right] \quad (33)$$

$$\gamma_{ikm} = \text{asin} [R_h \sin \theta_{ikm} / R_e] \quad (34)$$

$$G_{T_{ikm}} = \text{sinc}^2 \left[\pi \frac{\sin(\theta_{ikm} - \theta_m)}{\beta_{rm}} \right] \quad (35)$$

$$G_{R_{ikm}} = \text{sinc}^2 \left[\pi \frac{\sin(\theta_{ikm} - \theta_i)}{\beta_{ri}} \right] \quad (36)$$

where θ_m and θ_i are the central look angles of the m th and i th subswath, and β_{rm} and β_{ri} the range beamwidth of the m th and i th subswath.

Based on the radar equation and the definition of RASR, the RASR corresponding to the slant range R is

$$\text{RASR} = \frac{\sum_{m=0}^{N_{opt}-1} \sum_{\substack{k=-k_{im2} \\ (m=i, k \neq 0) \text{ or } (m \neq i)}}^{k_{im2}} \frac{\sigma_{ikm}^0 \cdot G_{T_{ikm}} \cdot G_{R_{ikm}}}{R_{ikm}^3 \sin \gamma_{ikm}}}{\left. \frac{\sigma_{ikm}^0 \cdot G_{T_{ikm}} \cdot G_{R_{ikm}}}{R_{ikm}^3 \sin \gamma_{ikm}} \right|_{m=i, k=0}} \quad (37)$$

Generally, the chosen PRF of the nearspace slow-moving borne SAR is bigger enough than Doppler bandwidth, so AASR is good enough. RASR degrades a little due to the interference of subswaths. However, the actual PRF is still very low, and RASR is good enough for practical systems.

4.3. Noise Equivalent Sigma Zero

Noise Equivalent Sigma Zero (NESZ) is an index about SNR of SAR images. Based on (4), NESZ corresponding to the slant range R is similar to those of conventional strip operation [1]. That is

$$\text{NESZ} = \left(\frac{\text{SNR}}{\sigma_0} \right)^{-1} = \frac{(4\pi)^3 R^4 F K T_n}{k_r k_a P_t \left(\frac{f_{p_{opt}}}{N_{opt}} \right) \tau_p G_t G_r \delta_a \delta_r T_s} \quad (38)$$

where $f_{p_{opt}}/N_{opt}$ is the equivalent PRF. Because the beamwidth is much narrower compared to a single wide range beam, the antenna gain is higher, and SNR of SAR images is higher. In other words, the transmitting power demand reduces.

5. DESIGN EXAMPLE

Consider a FA-ScanSAR system with the main parameters listed in Table 1. Azimuth resolution δ_a is 1.0 m, and the swath width Δ is 120 km. Let $k_1 = 1.09$ and $k_p = 1.2$, according to (6), $f_{p_{\min}} = 65.4$ Hz, and the corresponding AASR is -21.91 dB. If PRF is increased to 100 Hz, the corresponding AASR is -26.55 dB.

Table 1. Main parameters for FA-ScanSAR system.

Parameter	Value
Wavelength, λ	0.02 m
Height of the platform, h	25.0 km
Velocity of the platform, v	50.0 m/s
Look angle of the central swath, θ	75.0 deg
Length of pulse, τ_p	20 μ s
Bandwidth of LFM, B_w	200 MHz
Sample frequency, f_s	220 MHz
Peak power of transmitting, P_t	1000 w
System loss, F	2.6 dB
Noise temperature, T_n	817 K
Antenna efficiency, ρ	0.5

So we choose $f_{p_{\min}} = 100$ Hz for a better AASR and calculating convenience. Let $R_e = 6371$ km, according to (7)–(16), we can get $\alpha = 0.8634^\circ$, $g_{\min} = 36.004$ km, $\alpha_{\min} = 0.3238^\circ$, $\alpha_{\max} = 1.4030^\circ$, $R_{\min} = 43.89$ km, $R_{\max} = 158.29$ km, $f_{p_{\max}} = 930.0$ Hz, and $N_{\max} = 9$.

5.1. Results of System Parameters Design

For this example, the optimum swath number is selected $N_{opt} = 5$, and the width of each subswath $\Delta_i = 26.087$ km, which includes 10% overlap width. The actual PRF $f_{p_{opt}}$ is $N_{opt} \cdot f_{\min} = 500$ Hz, so the time period for transmitting pulse, receiving echo and switching beam of a subswath is 2.0 ms. The beam position parameters of the five subswaths are shown in Table 2. Form Table 2, we can see that there are at least 944.7 μ s left for beam switching.

5.2. Performance Contrast

Table 3 shows the azimuth resolution, AASR, RASR and NESZ of all subswaths for FA-ScanSAR. Furthermore, those performance

Table 2. Beam position parameters of the five subswaths.

Subswath sequence No.	Look angle Range (°)	Range beamwidth (°)	Ground range (km)	Echo window time (μs)	Sample points
1	55.116~67.828	12.712	36.00~62.09	292.6~447.0	33962
2	66.976~73.359	6.383	59.48~85.57	430.9~595.4	36191
3	72.888~76.622	3.734	82.96~109.0	578.7~747.2	37082
4	76.329~78.742	2.413	106.4~132.5	730.3~900.8	37513
5	78.545~80.212	1.667	129.9~156.0	883.7~1055.3	37749

Table 3. Performance parameters (azimuth resolution, AASR, RASR and NESZ) contrast for FA-ScanSAR, ScanSAR and convention strip operation.

Operation	Position	Central look angle (°)	Azimuth resolution (m)	AASR (dB)	RASR (dB)	NESZ (dB)
FA-ScanSAR	SW.1	61.472	1.0	-26.55	-64.65	-20.92
	SW.2	70.167	1.0	-26.55	-60.64	-22.33
	SW.3	74.755	1.0	-26.55	-69.53	-23.51
	SW.4	77.536	1.0	-26.55	-79.84	-24.53
	SW.5	79.379	1.0	-26.55	-57.26	-25.45
ScanSAR	SW.1	61.472	5.988	-26.55	/	-12.77
	SW.2	70.167	5.987	-26.55	/	-14.19
	SW.3	74.755	5.996	-26.55	/	-15.36
	SW.4	77.536	5.985	-26.55	/	-16.39
	SW.5	79.379	5.996	-26.55	/	-17.30
Conventional Strip	P.1	61.472	1.0	-26.55	/	-13.23
	P.2	70.167	1.0	-26.55	/	-10.16
	P.3	74.755	1.0	-26.55	/	-4.62
	P.4	77.536	1.0	-26.55	/	0.48
	P.5	79.379	1.0	-26.55	/	4.86

Notes: “SW.” represents the subswath for FA-ScanSAR and ScanSAR, and “P.” represents the position corresponding to the look angle for the conventional strip convention with a wide range beam. “/” represents that there is no ambiguous range area.

indexes are given for a ScanSAR with the same five subswaths and a conventional strip system with a wide beam. The burst numbers of the five subswaths of ScanSAR are 176, 250, 326, 404 and 481 respectively. The AASR values of the central positions are listed for ScanSAR only.

According to the results in Table 3, we can see FA-ScanSAR proposed in this paper can obtain the same azimuth resolution and AASR with the convention strip operation, and RASR increases but is still small enough for general application. It must be pointed out that NESZ of FA-ScanSAR is much better than those of ScanSAR and conventional strip operation. This operation can reduce the transmit power demand.

6. CONCLUSION

Considering the characteristic of low PRF for the nearspace slow-moving platform, syncretizing the principles of ScanSAR and the conventional strip, a novel operation — FA-ScanSAR is proposed for high resolution imaging in wide swath. This operation can obtain full aperture accumulation in all the subswaths, and the low gain of wide beamwidth is avoided. So the better NESZ of FA-ScanSAR is helpful for the realization of SAR system. The design example shows that FA-ScanSAR is a feasible operation for high resolution and wide swath imaging.

ACKNOWLEDGMENT

This research is supported by China Postdoctoral Science Foundation.

REFERENCES

1. Curlander, J. C. and R. N. McDonough, *Synthetic Aperture Radar Systems and Signal Processing*, Wiley Series in Remote Sensing, John Wiley & Sons, 1991.
2. Currie, A. and M. A. Brown, "Wide-swath SAR," *IEE Proceedings*, Vol. 139, No. 2, 122–135, April 1992,
3. Younis, M., "Digital beam-forming for high resolution wide swath real and synthetic aperture radar," Doctoral dissertation, University of Karlsruhe, July 2004.
4. Freeman, A., G. Krieger, P. Rosen, et al., "SweepSAR: Beam-forming on receive using a reflector-phase array feed combination for spaceborne SAR," *Proc. of 2009 IEEE Radar Conference*, 1–9, Pasadena, USA, May 4–8, 2009.

5. Moore, R. K., J. P. Classsem, and Y. H. Lin, "Scanning spaceborne synthetic aperture radar with integrated radiometer," *IEEE Trans. on Aerosp. Electron. Syst.*, Vol. 17, No. 3, 410–420, May 1981.
6. De Zan, F. and A. M. Guarnieri, "TOPSAR: Terrain observation by progressive scans," *IEEE Trans. Geosci. Remote Sensing*, Vol. 44, No. 9, 2352–2360, September 2006.
7. Carrara, W. G., R. S. Goodman, and R. M. Majewski, *Spotlight Synthetic Aperture Radar*, Artech House, Boston, 1995.
8. Callaghan, G. D., "Wide swath SAR: Overcoming the trade-off between swath and azimuth resolution," Doctoral Dissertation, Queensland Univ., Brisbane, Australia, 1999.
9. Li, Z. F., H. Y. Wang, T. Su, et al., "Generation of wide-swath and high-resolution sar images from multichannel small spaceborne SAR systems," *IEEE Geosci. Remote Sensing Letters*, Vol. 2, No. 1, 82–86, January 2005.
10. Gebert, N. and G. Krieger, "Azimuth phase center adaptation on transmit for high-resolution wide-swath SAR imaging," *IEEE Geosci. Remote Sensing Letters*, Vol. 6, No. 4, 782–786, October 2009.
11. Freeman, A., A. Donnellan, P. Rosen, et al., "Deformation, ecosystem structure, and dynamics of ice (DESDynI)," *Proc. of EUSAR*, Vol. 2, 115–118, Friedrichshafen, Germany, June 2–5, 2008.
12. Allen, E. H., "The case for near space," *Aerospace America*, 31–34, February 2006.
13. Bolkcom, C., "Potential military use of airships and aerostats," *CRS Report for Congress*, RS211886, November 11, 2004.
14. Weeks, D. J., S. H. Walker, and R. L. Sackheim, "Small satellites and the DARPA/Air force FALCON program," *Acta Astronautica*, Vol. 57, 469–277, 2005.
15. Wang, W. Q., J. Y. Cai, and Q. C. Peng, "Near-space SAR: A revolutionizing remote sensing mission," *Proc. of APSAR Conf.*, 127–131, Huangshan, China, 2007.
16. Wang, W. Q., Q. C. Peng, J. Y. Cai, and L. Wang, "Azimuth signal processing for near-space high-resolution and wide-swath imaging," *Proc. of ICSP*, 2330–2332, 2008.
17. Wang, W. Q., J. Y. Cai, and Q. C. Peng, "Near-space microwave radar remote sensing: Potentials and challenge analysis," *Remote Sensing*, Vol. 2, 717–739, 2010.